

## RESIK OBSERVATIONS OF HELIUM-LIKE ARGON X-RAY LINE EMISSION IN SOLAR FLARES

J. SYLWESTER AND B. SYLWESTER

Space Research Centre, Polish Academy of Sciences, 51-622, Kopernika 11, Wrocław, Poland; js@cbk.pan.wroc.pl

AND

K. J. H. PHILLIPS

UCL-Mullard Space Science Laboratory, Holmbury St Mary, Dorking, Surrey RH5 6NT, UK; kjhp@mssl.ucl.ac.uk

Received 2008 April 17; accepted 2008 June 3; published 2008 June 25

### ABSTRACT

The Ar xvii X-ray line group principally due to transitions  $1s^2-1s2l$  ( $l = s, p$ ) near 4 Å was observed in numerous flares by the RESIK bent crystal spectrometer aboard *CORONAS-F* between 2001 and 2003. The three line features include Ar xvii  $w$  (resonance line), a blend of  $x$  and  $y$  (intercombination lines), and  $z$  (forbidden line), all of which are blended with Ar xvi dielectronic satellites. The ratio  $G$ , equal to  $[I(x) + I(y) + I(z)]/I(w)$ , varies with electron temperature  $T_e$  mostly because of unresolved dielectronic satellites. With temperatures estimated from *GOES* X-ray emission, the observed  $G$  ratios agree fairly well with those calculated from CHIANTI and other data. With a two-component emission measure, better agreement is achieved. Some S xv and S xvi lines blend with the Ar lines, the effect of which occurs at temperatures  $\geq 8$  MK, allowing the S/Ar abundance ratio to be determined. This is found to agree with coronal values. A nonthermal contribution is indicated for some spectra in the repeating-pulse flare of 2003 February 6.

*Subject headings:* line: identification — Sun: abundances — Sun: corona — Sun: flares — Sun: X-rays, gamma rays

### 1. INTRODUCTION

High-resolution soft X-ray spectral observations have provided important information about the physical properties of solar flares and active regions, including electron temperatures  $T_e$ , densities  $N_e$ , and ionization state. Those from the bent crystal spectrometer RESIK (REntgenovsky Spektrometr s Izognutymi Kristalami) on the Russian *CORONAS-F* spacecraft (Sylwester et al. 2005b) cover the range 3.3–6.1 Å, which includes strong emission lines of Si, S, and Ar ions and continuum and also weaker lines of Cl and K ions. The wavelength resolution  $\Delta\lambda$  is between 8 mÅ (3.4 Å) and 17 mÅ (6.1 Å). The instrument operated successfully between 2001 (shortly after the launch of *CORONAS-F* on July 31) and 2003 May, obtaining numerous flare and active-region spectra. RESIK spectra have already been used for K, Ar, Cl, S, and Si abundance determinations in flares (Sylwester et al. 2006). Lines in the 3.3–6.1 Å range have not been well observed by previous spectrometers with the exception of the He-like S (S xv) lines at  $\sim 5$  Å. Of particular interest here are the He-like Ar (Ar xvii) lines between 3.94 Å and 4.00 Å and associated dielectronic satellites emitted by Li-like Ar (Ar xvi). There are four prominent Ar xvii lines, due to transitions from the  $1s2p\ ^1P_1$ ,  $1s2p\ ^3P_2$ ,  $1s2p\ ^3P_1$ , and  $1s2s\ ^3S_1$  levels to the ground level  $1s^2\ ^1S_0$  (designated lines  $w$ ,  $x$ ,  $y$ , and  $z$  respectively), with wavelengths 3.949, 3.966, 3.969, and 3.994 Å. Dielectronic Ar xvi satellites, particularly  $q$  (3.981 Å),  $k$  (3.990 Å), and  $j$  (3.994 Å), feature prominently.

The Ar xvii lines have been observed during a few solar flares with the Flat Crystal Spectrometer (FCS) on *Solar Maximum Mission*, with the Ar xvi  $k$  satellite being resolved from the Ar xvii line  $z$  but with  $j$  indistinguishable from line  $z$ . RESIK flare spectra do not resolve lines  $k$  and  $z$  or the Ar xvii  $x$  and  $y$  lines, so there are three main features, the blend of line  $w$  with unresolved weak Ar xvi satellites on the long-wavelength side of  $w$  ( $w'$ ), the blend of lines  $x$ ,  $y$ , and other weak Ar xvi satellites  $[(x+y)']$ , and the blend of line  $z$  with the two prominent satellites  $j$  and  $k$  ( $z'$ ). The relative fluxes of these three line features can thus be examined over a variety

of flare conditions, owing to RESIK's sensitivity being much improved (by a factor  $\sim 60$ ) over the FCS. In particular, the temperature dependence of the ratio  $G$ , which in terms of the observed features is  $[I(x+y)' + I(z')]/I(w')$ , can be examined. At temperatures  $\geq 8$  MK, the effect of sulphur lines blending with the three Ar xvii line features becomes apparent on the  $G$  ratio. These are the  $1s-3p$  (Ly $\beta$ ) line of S xvi (3.991 Å) and the  $1s^2-1s5p$  line of S xv (3.998 Å) blending with the Ar xvii  $z$  line, and the  $1s^2-1s6p$  line of S xv (3.949 Å) blending with the Ar xvii  $w$  line. These lines were not considered in an earlier analysis of FCS spectra (Phillips et al. 1993).

### 2. OBSERVATIONS

The observations analyzed here were made with channel 2 of RESIK (nominal range for an on-axis source 3.83–4.27 Å), for which the diffracting crystal is Si 111 ( $2d = 6.27$  Å). A 0.5% background due to fluorescence of the crystal material for this channel has been completely accounted for. During a flare, spectra are recorded in data-gathering intervals (DGIs) that are adjustable according to the X-ray flux. For a typical *GOES*-class M1 flare, the DGI may be from several minutes at the start and end of the flare to  $\sim 2$  s at flare peak. Some 1500 spectra during seven flares of various importance are available, from which 98 flare maxima or postmaxima spectra were selected and analyzed in detail. Details of the time periods and flare importance are given in Table 1. These spectra have been processed to account for all known instrumental effects.<sup>1</sup> Spectra during the rise of the flare of 2003 February 6 are shown in Figure 1 (*upper panel*). Gaussian profiles to the main line features  $w'$ ,  $(x+y)'$ , and  $z'$  were fitted using a nonlinear least-squares fitting procedure with an arbitrary number of parameters available in a library of Interactive Data Language (IDL) procedures. The output consists of estimated fluxes with

<sup>1</sup> The data are made available to the solar physics community through the Web site [http://www.cbk.pan.wroc.pl/RESIK\\_Level2](http://www.cbk.pan.wroc.pl/RESIK_Level2) based at the Space Research Centre, Wrocław, Poland.

TABLE 1  
ANALYZED RESIK FLARE SPECTRA

Date	Time Range of RESIK Spectra (UT)	Time of Maximum GOES (1–8 Å) Flux	GOES Class
2002 Oct 4 .....	05:39–05:54	05:38	M4.0
2002 Dec 17 .....	23:08–23:19	23:09	C6.1
2003 Jan 7 .....	23:36–23:43	23:33	M4.9
2003 Jan 9 .....	01:36–02:08	01:39	C9.8
2003 Feb 1 .....	09:12–10:14	09:06	M1.2
2003 Feb 6 .....	02:09–02:31	02:12	C3.2
2003 Feb 22 .....	04:50–05:02	05:10	B9.6

uncertainties of the three observed features, from which  $G$  ratios with uncertainties can be derived. Fits to one of the spectra in the upper panel of Figure 1 are shown in the lower panel.

Temperatures over the period of each spectrum were estimated from the flux ratio of the two channels (0.5–4 Å and 1–8 Å) of *GOES*. In this procedure, standard IDL routines were used to derive the temperatures which are based on the flux sensitivity of the *GOES* channels and model X-ray spectra calculated with version 5.2 of the CHIANTI atomic database and spectral code (Landi et al. 2006). The routines are from White et al. (2005) in which account is taken of differing coronal and photospheric element abundances. Temperatures were derived here using coronal abundances (later we show that the coronal Ar/S abundance ratio fits our data better), but for the temperature range of RESIK spectra analyzed in this work (5–16 MK) the temperature differences using coronal and photospheric abundances are very small, between 0.9 and 0.5 MK, in agreement with White et al. (2005).

As well as RESIK spectra, four *SMM* FCS spectra during flares in 1988 were included in the analysis, as listed by Phillips et al. (1993). As the spectra were scanned in each case, the different Ar XVII lines were observed at slightly different times, unlike the RESIK spectra which are formed simultaneously, but the scan times were only 3 minutes, short enough that insignificant time variations occurred. In addition, a laboratory spectrum of the Ar XVII lines (Bitter et al. 2003) was included in the data. The spectrum in this case was taken during ohmically heated discharges from the National Spherical Torus Experiment (NSTE), with temperature measured from Thomson scattering. The electron densities are much higher ( $5 \times 10^{13} \text{ cm}^{-3}$ ) than those expected in flares, but the comparison of the  $G$  ratio should still be valid as it is a function of  $T_e$  alone.

### 3. ATOMIC CALCULATIONS

For He-like ion lines, the ratio  $G = [I(x) + I(y) + I(z)]/I(w)$  is slightly sensitive to electron temperature  $T_e$  owing to the different energy dependence of the collisional excitation rate coefficients from the ground state to the upper levels of each line (Gabriel & Jordan 1969). The theoretical temperature dependence of the Ar XVII  $G$  ratio used here is based on data in the CHIANTI atomic database (ver. 5.2), taken from Zhang & Sampson (1987). This is shown in Figure 2 (*lower panel, solid line*). The effect of Ar XVI dielectronic satellites on the  $G$  ratio is of major consequence. Satellites with transitions  $1s^2 nl-1s2l nl'$  ( $n \geq 3$ ) converge on and blend with lines  $w$  and  $y$ , while the prominent satellites  $j$  and  $k$  (with  $n = 2$ ) blend with line  $z$ . The contribution functions (fluxes per unit emission measure) of all the  $n = 2$  and  $n = 3$  satellites for different temperatures were taken from CHIANTI. The combined effect of higher- $n$  satellites ( $n \geq 4$ ) is also important, but in the ab-

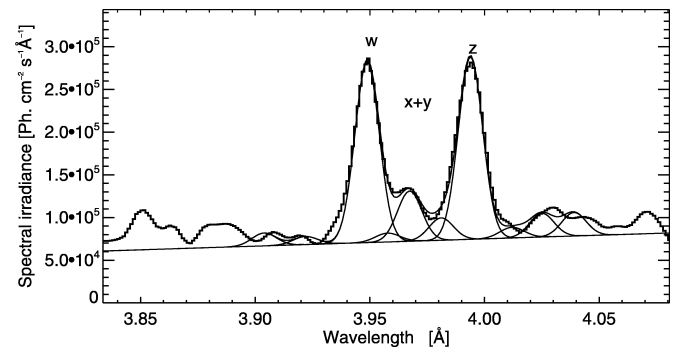
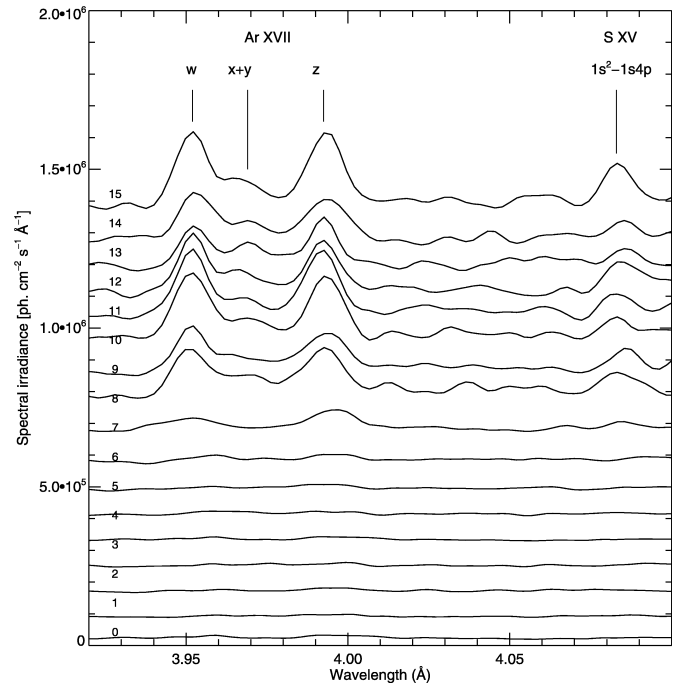


FIG. 1.—*Upper panel*: Examples of RESIK spectra in the 3.85–4.07 Å region including the Ar XVII lines described in the text and the S XV  $1s^2-1s4p$  line at 4.089 Å. They cover the period 02:00:44–02:12:08 UT extending over the rise phase to the first maximum of the 2003 February 6 flare. Spectra are stacked with times increasing upward. *Lower panel*: Gaussian fits to the RESIK spectrum at 02:10:47–02:11:03 UT (spectrum 11) illustrating the line-fitting procedure (with the IDL routine *lmfit*). Only the line features  $w$ ,  $x + y$ , and  $z$  are real.

sence of any available data, their contribution was estimated from factors for equivalent Fe XXIV satellites (Bely-Dubau et al. 1979). The effect of all Ar XVI satellites on the observed  $G$  ratio ( $G'$ ) is shown in Figure 2 (*lower panel, dashed line*). Note that for much of the temperature range shown,  $\log T_e = 6.7-7.2$ , the He-like stage  $\text{Ar}^{+16}$  dominates over all other Ar ionization stages (Mazzotta et al. 1998).

The effect on the  $G$  ratio of S XV and S XVI lines was estimated from CHIANTI. The S XVI  $1s-3p$  ( $\text{Ly}\beta$ ) line at temperatures  $\geq 8$  MK, blending with the Ar XVII  $z$  line, is particularly important, tending to increase  $G$ . The exact effect of the S lines on  $G$  depends on an assumed S/Ar abundance ratio, which for coronal abundances (Feldman et al. 1992) is 4.9 but for photospheric abundances (Grevesse & Sauval 1998) is 8.5. The dash-double-dotted ( $G''_{\text{cor}}$ ) and dash-dotted curves ( $G''_{\text{phot}}$ ) show the effect of the S lines on  $G$  for coronal and photospheric abundances, respectively. The difference between the two curves is sufficiently large at  $T_e \geq 12$  MK that RESIK flare

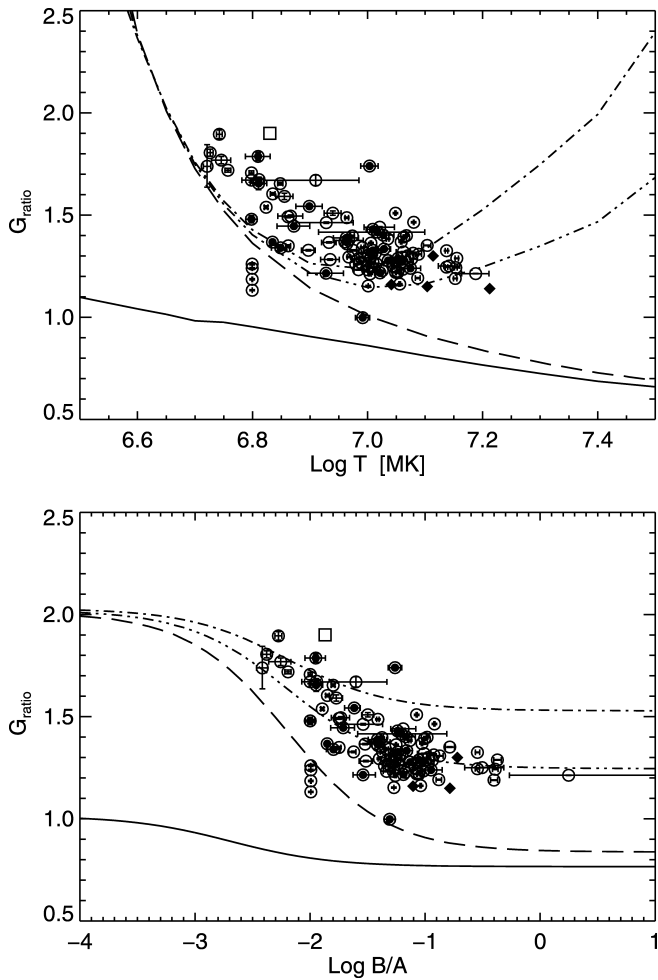


FIG. 2.—*Upper panel:* The Ar XVII  $G$  ratio plotted against  $\log T_e$  in an isothermal approximation. For theoretical calculations, the solid line is  $G = [I(x) + I(y) + I(z)]/I(w)$  for the Ar XVII lines alone, the dashed line is  $G$  including Ar XVI satellites, the dash-double-dotted line is  $G$  including S XV and S XVI lines for coronal Ar/S abundance ( $G''_{\text{cor}}$ ), and the dash-dotted line includes the S lines with photospheric Ar/S abundance ( $G''_{\text{phot}}$ ). Observational points (circles with small error bars) are measured  $G$  for spectra during flares (Table 1), with filled circles for spectra during the 2003 February 6 flare. The filled diamonds are for the *SMM* FCS spectra. Temperatures  $T$  are electron temperatures for the theoretical curves and for the observational points are derived from the ratio of the two *GOES* channels. The square is for the NSTE tokamak Ar XVII spectrum, with temperatures from Thomson scattering (Bitter et al. 2003). *Lower panel:* The Ar XVII  $G$  ratio plotted against  $\log(B/A)$  for a two-component DEM =  $A\delta(T_1) + B\delta(T_2)$  with  $T_1 = 4.5$  MK and  $T_2 = 16$  MK. The line styles and symbols for the observed points are the same as above.

spectra can be expected to distinguish between coronal and photospheric abundances for flares.

#### 4. RESULTS

The observed  $G$  ratios, defined by  $G = [I(x + y)' + I(z)']/I(w')$  from estimated fluxes of the Ar XVII line features  $w'$ ,  $(x + y)'$ , and  $z'$ , are plotted in Figure 2 (*upper panel*) against temperatures from the flux ratio of the two *GOES* channels. The points (including the RESIK nonflaring point, *SMM* FCS points, and the NSTE tokamak point of Bitter et al. 2003) follow a clear trend with temperature, although there is a general displacement of the observed  $G$  ratios from the theoretical curves  $G''_{\text{cor}}$  (Ar XVII  $G$  ratio with S lines, coronal Ar/S abundance ratio) such that either the *GOES* temperatures are too low (by 0.1 in  $\log T_{\text{GOES}}$ ) or the ratios are  $\sim 20\%$  too low. A

similar effect was obtained for ratios of dielectronic satellites to Si XIII  $1s^2 \ ^1S_0 - 1snp \ ^1P_1$  ( $n = 3, 4$ ) lines observed by RESIK (Phillips et al. 2006), which was attributed to nonisothermal plasma in the flare. In general, a flare plasma is expected to have a differential emission measure (DEM)  $\varphi(T_e) = N_e^2 dV/dT_e$  extending over a broad temperature range, up to  $T_e \sim 20 \times 10^6$  K for M and X flares. The value of  $G$  can be derived from the dependence on  $T_e$  of the DEM, which in principle can be found from several X-ray emission lines (e.g., Sylwester et al. 1980; Keça et al. 2006). In previous work we have used simple forms for the DEM with some success, e.g., DEM = constant  $\times \exp(-T_e/T_0)$  ( $T_0 = \text{constant}$  for each spectrum, calculable from the ratio of the emission in the two *GOES* channels). This gave a fair agreement of observed and theoretical Si XII/Si XIII line ratios (Phillips et al. 2006). For this analysis, however, analytic forms were not so satisfactory, and instead, a two-component emission measure was found to give the best agreement with the observations, with DEM given by the weighted sum of two delta functions, DEM =  $A\delta(T_1) + B\delta(T_2)$ , with the temperatures  $T_1$  and  $T_2$  being constant for all spectra but  $A$  and  $B$  being variable. This form of the DEM has been found to give satisfactory results for other data (Sylwester et al. 2005a), and although its use here is more for convenience in the analysis, physical importance might be attributed to the two temperatures in that  $T_1$  appears to represent the nonflaring active region temperature and  $T_2$  the temperature of the flare proper. The theoretical  $G$  ratios, with and without the Ar XVI satellites and the sulphur lines, are plotted against  $\log(B/A)$  in Figure 2 (*lower panel*) for the case of  $T_1 = 4.5$  MK and  $T_2 = 16$  MK. These values give the best agreement of the observed points and the theoretical curves; in particular, the point of inflection between the low- and high-temperature asymptotic values of the  $G''_{\text{cor}}$  curve best matches that in the observed points.

Values of  $\log(B/A)$  for the observed  $G$  ratios were obtained from the emission ratio of the two *GOES* channels using the DEM delta-function form with  $T_1 = 4.5$  MK and  $T_2 = 16$  MK. These are shown in Figure 2 (*lower panel*). There is now improved agreement with the  $G''_{\text{cor}}$  curve (coronal S/Ar abundance ratio). Values of  $B/A$  range from 0.003 to 1.6, i.e., DEMs with the  $T_1 = 4.5$  MK component dominant to DEMs in which the two components are comparable to each other.

For the 2003 February 6 flare, the Ar XVII  $x + y$  or  $z$  line feature has anomalously high flux compared with the  $w$  line for two spectra, giving  $G \sim 1.7$ . For the  $G''_{\text{cor}}$  curve, this is expected only for very low (5 MK) or high (18 MK) temperatures, but the *GOES* temperatures for these time periods are 8–10 MK. In Figure 2,  $G$  for these spectra are thus well above the cluster of points. This flare is of particular interest because its light curve in X-rays up to energies of 25 keV, as shown by *RHESSI* observations, consists of seven semiperiodic pulses that originate in active regions on either side of the solar equator, linked by a transequatorial loop. Foullon et al. (2005) discuss the excitation of individual pulses in terms of a fast magnetoacoustic kink mode excited in the transequatorial loop. RESIK observations cover the period 02:03–02:17 UT, the period of the first two pulses. One of the anomalous  $G$  ratios occurs at 02:09 UT when an impulsive burst in the *RHESSI* 12–25 keV range occurs, about 85 s before the peak of the first pulse. The  $G$  ratio is high because the  $z'$  line feature is high relative to the other Ar XVII lines, and it is possible that  $z'$  is enhanced because of the high fluxes of the Ar XVI  $j$  and  $k$  satellites which blend with the Ar XVII  $z$  line. The upper levels of these lines are excited by electrons with energy 2.2

keV, so their enhancement may be due to an overabundance of electrons with this energy. The time coincidence with the 12–25 keV X-ray pulse would then suggest a nonthermal component of the Ar XVII emission.

Both panels of Figure 2 indicate a much clearer agreement of the observed  $G$  ratios with the  $G''_{\text{cor}}$  curve, i.e., with coronal S/Ar abundance (4.9: Feldman et al. 1992), than the  $G''_{\text{phot}}$  curve with photospheric S/Ar abundance (8.5: Grevesse & Sauval 1998). This points to the origin of the flare plasmas in the RESIK sample being coronal. According to Feldman & Laming (2000), flare plasmas have coronal abundances unless very impulsive when photospheric abundances appear to be present. This accords with our analysis since the flares observed (Table 1) are all gradual in character.

## 5. CONCLUSIONS

We have discussed RESIK observations of the  $G$  ratio for the Ar XVII lines at  $\sim 4 \text{ \AA}$  over a wide range of activity. For

98 flare spectra as well as four *SMM* FCS spectra, there is a clear trend of  $G$  that is close to the theoretical ratio. The agreement is improved for a two-component DEM. From this it is deduced that the Ar/S abundance ratio is close to 4.9, its coronal value, thus indicating a coronal origin for the flare plasma. Two spectra with anomalous  $G$  during the 2003 February 6 flare are noted, one of which is exactly at the time of an impulsive, nonthermal burst in *RHESSI* 12–25 keV emission. There is thus some suggestion that part of the Ar XVII emission is non-thermal in origin.

We thank the Polish Ministry of Science and Education for financial support from grant 1 P03D 017 29 and travel support from a UK Royal Society/Polish Academy of Sciences International Joint Project. CHIANTI is a collaborative project involving NRL (USA), MSSL (UK), the Universities of Florence (Italy) and Cambridge (UK), and George Mason University (USA).

## REFERENCES

- Bely-Dubau, F., Gabriel, A. H., & Volonté, S. 1979, *MNRAS*, 189, 801  
 Bitter, M., et al. 2003, *Phys. Rev. Lett.*, 91(26), 5001  
 Feldman, U., & Laming, J. M. 2000, *Phys. Scr.*, 61, 222  
 Feldman, U., Mandelbaum, P., Seely, J. F., Doschek, G. A., & Gursky, H. 1992, *ApJS*, 81, 387  
 Foullon, C., Verwichte, E., Nakariakov, V. M., & Fletcher, L. 2005, *A&A*, 440, L59  
 Gabriel, A. H., & Jordan, C. 1969, *MNRAS*, 145, 241  
 Grevesse, N., & Sauval, A. J. 1998, *Space Sci. Rev.*, 85, 161  
 Kępa, A., Sylwester, J., Sylwester, B., Siarkowski, M., & Stepanov, A. I. 2006, *Sol. Syst. Res.*, 40, 294  
 Landi, E., Del Zanna, G., Young, P. R., Dere, K. P., Mason, H. E., & Landini, M. 2006, *ApJS*, 162, 261  
 Mazzotta, P., Mazzitelli, G., Colafrancesco, S., & Vittorio, N. 1998, *A&AS*, 133, 403  
 Phillips, K. J. H., Dubau, J., Sylwester, J., & Sylwester, B. 2006, *ApJ*, 638, 1154  
 Phillips, K. J. H., Harra, L. K., Keenan, F. P., Zarro, D. M., & Wilson, M. 1993, *ApJ*, 419, 426  
 Sylwester, J., Schrijver, J., & Mewe, R. 1980, *Sol. Phys.*, 67, 285  
 Sylwester, J., Sylwester, B., Landi, E., Phillips, K. J. H., & Kuznetsov, V. D. 2006, *Adv. Space Res.*, 36, 2871  
 Sylwester, J., Sylwester, B., Phillips, K. J. H., & Kępa, A. 2005a, in *The Dynamic Sun: Challenges for Theory and Observations*, ed. D. Danesy et al. (ESA SP-600E; Noordwijk: ESA), 143  
 Sylwester, J., et al. 2005b, *Sol. Phys.*, 226, 45  
 White, S. M., Thomas, R. J., & Schwartz, R. A. 2005, *Sol. Phys.*, 227, 231  
 Zhang, H., & Sampson, D. H. 1987, *ApJS*, 63, 487